Human Molecular Genetics, 2012, Vol. 21, No. 15 **3356–3365**
doi:10.1093/hmg/dds167
Advance Access published on April 27, 2012

Reticulon-like-1, the *Drosophila* orthologue of the Hereditary Spastic Paraplegia gene reticulon 2, is required for organization of endoplasmic reticulum and of distal motor axons

Niamh C. O'Sullivan[1,*], Thomas R. Jahn[1], Evan Reid[2] and Cahir J. O'Kane[1,*]

[1]Department of Genetics and [2]Cambridge Institute for Medical Research and Department of Medical Genetics, University of Cambridge, Cambridge CB2 3EH, UK

Received March 21, 2012; Revised and Accepted April 20, 2012

Several causative genes for hereditary spastic paraplegia encode proteins with intramembrane hairpin loops that contribute to the curvature of the endoplasmic reticulum (ER), but the relevance of this function to axonal degeneration is not understood. One of these genes is *reticulon2*. In contrast to mammals, *Drosophila* has only one widely expressed reticulon orthologue, *Rtnl1*, and we therefore used *Drosophila* to test its importance for ER organization and axonal function. Rtnl1 distribution overlapped with that of the ER, but in contrast to the rough ER, was enriched in axons. The loss of Rtnl1 led to the expansion of the rough or sheet ER in larval epidermis and elevated levels of ER stress. It also caused abnormalities specifically within distal portions of longer motor axons and in their presynaptic terminals, including disruption of the smooth ER (SER), the microtubule cytoskeleton and mitochondria. In contrast, proximal axon portions appeared unaffected. Our results provide direct evidence for reticulon function in the organization of the SER in distal longer axons, and support a model in which spastic paraplegia can be caused by impairment of axonal the SER. Our data provide a route to further understanding of both the role of the SER in axons and the pathological consequences of the impairment of this compartment.

INTRODUCTION

Hereditary spastic paraplegias (HSPs) are a group of neurological disorders characterized by retrograde degeneration of long nerve fibres in the corticospinal tracts and posterior columns, sometimes accompanied by additional, mainly neurological symptoms (1,2). The disease mechanisms are largely unknown, but since distal regions of longer axons appear to be worst affected, the disease may reflect problems in trafficking cell components between the cell body and distal axons that can be up to a metre away. Some clues about disease mechanisms come from the identification of over 20 causative HSP genes (SPGs, spastic paraplegia genes) (3). These encode a heterogeneous group of proteins, but the largest single class are intracellular membrane proteins, principally the endosomal or endoplasmic reticulum (ER). Functions ascribed to these proteins (not mutually exclusive) include the inhibition of BMP signalling (4–6), formation of lipid droplets (7–9) or regulation of ER topology (10–13).

At least four autosomal dominant HSPs are caused by mutations in proteins that have a common feature of ER localization, and an intramembrane hairpin loop that can induce or sense the curvature of ER membranes and form oligomeric complexes among themselves and each other (10–15). These hairpin-loop proteins, SPG3A/atlastin1, SPG4/spastin, SPG12/reticulon2 (RTN2) and SPG31/REEP1, contribute to ER topology in a number of ways. Reticulon and REEP proteins share a partly redundant role in the formation of tubular ER, and in the induction of the curvature at the edges of the sheet ER (10,16). ER tubule elongation is proposed to in-

*To whom correspondence should be addressed. Tel: +44 1223333177; Fax: +44 1223333992; Email: c.okane@gen.cam.ac.uk (C.J.O'K); n.osullivan@gen.cam.ac.uk (N.C.O'S)

volve both REEP proteins and the microtubule (MT)-severing activity of spastin, which could potentially nucleate new MT elongation and accompanying tubule extension (13,17–19). The GTPase Atlastin1 is thought to mediate the membrane fusion events that maintain the reticular organization of the ER (12,14,20).

Little protein synthesis occurs in axons (21), and consequently they contain very little rough ER (RER) (22); it is at first sight paradoxical that mutations in ER-modelling proteins could be causative for axonal degeneration. However, axons and presynaptic terminals contain the smooth ER (SER), based on ultrastructural evidence and the presence of calcium homeostasis machinery (22–26). Since smooth and tubular ER are broadly equivalent (16), this could explain why axons are sensitive to mutations in proteins that model tubular ER.

One of the major ER-tubulating protein classes is the reticulon family, one of whose members, RTN2, was recently identified as an *SPG* gene product (15). Here, we used *Drosophila* to test the effects on the ER and axons of the loss of reticulon function. *Drosophila* has a single widely expressed reticulon, reticulon1 (Rtnl1), that is an orthologue of reticulons 1–4 in humans. We show that Rtnl1 is required for ER network organization, and that its loss induces an ER stress response. Furthermore, the loss of Rtnl1 leads to abnormalities of an SER marker, the MT cytoskeleton and mitochondria, in the distal axons or presynaptic termini of longer motor axons. Our findings reveal increased susceptibility of posterior axons to the disruption of ER organization and suggest a mechanism by which the loss of hairpin loop proteins gives rise to axonopathy.

RESULTS

Loss of Rtnl1, the *Drosophila* orthologue of vertebrate reticulons 1–4, causes age-related locomotor deficits

Drosophila has two reticulons, *Rtnl1* and *Rtnl2*, that are orthologous to the four reticulons found in mammals (Fig. 1A) (27,28). We focused on *Rtnl1* as most relevant to the function of its mammalian orthologues. *Rtnl1* is widely expressed, whereas *Rtnl2* expression is restricted to testis and fat body (www.flyatlas.org); moreover, BLASTP searches (not shown) show that *Rtnl1* is evolving more slowly than *Rtnl2*, suggesting that its function is better conserved.

An *Rtnl1* exon trap insertion tagged with yellow fluorescent protein (YFP) (Fig. 1B) showed widespread expression in third-instar larvae, with the highest levels observed in neural tissues. Its subcellular localization was seen most clearly in epidermal cells, where it had a reticular distribution, overlapping with labelling of the ER retention signal KDEL (Fig. 1C). In contrast, in the CNS, relatively low levels of Rtnl1::YFP were found in cell bodies where most KDEL labelling is found (Fig. 1D); much higher levels were found in the neuropil (containing axons, dendrites and synapses) and in the nerves that connect the CNS to the periphery, which include motor neuron axons. In motor neuron terminals at the neuromuscular junction (NMJ), Rtnl1::YFP followed the distribution of the axonal MT marker Futsch (homologous to mammalian MAP1B), consistent with the established close association of tubular ER and MTs (Fig. 1E) (13,29). Therefore, Rtnl1::YFP overlaps with the ER, but its distinct distribution in neurons suggests that a smooth tubular ER compartment, marked by Rtnl1::YFP, is found preferentially in axons rather than in cell bodies.

To detect whether the loss of Rtnl1 had any overt phenotypic consequences, we tested for any obvious effects of ubiquitous knockdown of *Rtnl1*, using an RNAi insertion expressed under the control of *da-Gal4*, which resulted in almost complete depletion of *Rtnl1* (Fig. 1F). Rtnl1 knockdown flies were viable, and an automated three-dimensional tracking system that measured the climbing behaviour of these flies in a negative geotaxis assay (30) showed that they had normal locomotor activity as early adults (Fig. 1G and H). However, as adults aged, they showed a progressive loss of locomotor activity relative to controls (Fig. 1G and H), consistent with a degenerative phenotype caused by Rtnl1 loss.

Rtnl1 is required for normal ER organization and function

In vitro studies have shown that reticulon proteins are required for tubular ER formation and maintenance (10,16). We therefore investigated the effects of *Rtnl1* knockdown on ER organization *in vivo*. The loss of Rtnl1 made the perinuclear pattern of KDEL labelling in epidermal cells more diffuse than the reticular pattern seen in controls, but did not detectably change the overall levels of KDEL labelling (Fig. 2A). In contrast, the distribution of the Golgi marker GM130 was not detectably changed in *Rtnl1* knockdown epidermal cells (Fig. 2A). Ultrastructural analysis revealed that the diffuse KDEL labelling in epidermal cells of *Rtnl1* knockdown larvae was caused by a striking reorganization of the ER, including a 3-fold increase in the average length of sheet ER profiles, and denser packing of the ribosomal studded sheet ER (Fig. 2B). This could result either from the loss of the curved edges of the sheet ER, to which reticulons contribute (16), or from the conversion of highly curved tubular ER to the sheet ER.

The main signalling mechanism controlling ER homeostasis, including the size and the shape, is the ER unfolded protein response (31). This induces expression of a large number of genes that encode components of the ER-resident folding machinery, stimulate lipid biosynthesis and enlarge the ER (32). We therefore tested whether the expansion of ER sheets observed in *Rtnl1* knockdown larvae coincided with an ER stress response, using the ER stress reporter Xbp1::enhanced green fluorescent protein (EGFP) in which EGFP is expressed in frame with Xbp1 only after ER-stress activated splicing occurs (33). *Rtnl1* knockdown significantly increased the ER stress response compared with controls, both in epidermal cells and neurons (Fig. 2C and D).

Loss of Rtnl1 leads to defects in longer motor axons

Given that spastic paraplegia mutations lead to axonal degeneration, we wanted to test for tubular ER defects in axons of *Rtnl1* knockdown larvae. Since most commonly used ER markers are associated with protein synthesis, traffic or folding, which occurs mainly in the RER in neuronal cell bodies, we set out to identify markers of the SER by identification of Rtnl1::YFP interactors, using mass-spectroscopy,

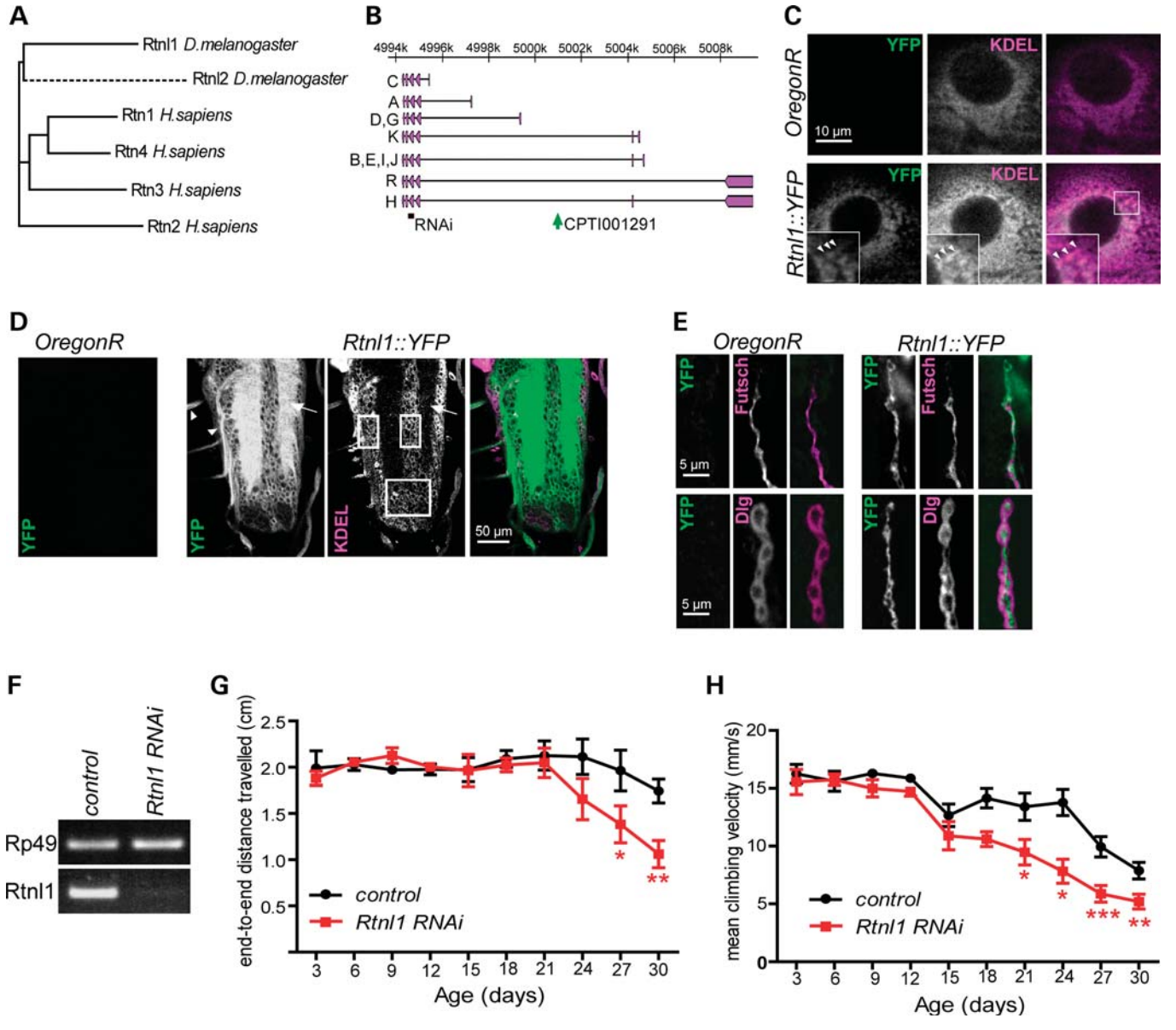

Figure 1. Loss of *Drosophila* reticulon causes a progressive locomotor deficit. (**A**) Dendrogram showing similarity of human and *Drosophila* reticulon proteins, drawn from a Clustal alignment using the neighbour-joining algorithm in MEGA 5.05. Dashed line indicates fast divergence of *Drosophila* Rtnl2. (**B**) The *Rtnl1* locus showing proteins encoded by transcripts A-R (Flybase Genome Browser R5.41), location of VDRC RNAi fragments (RNAi) and the Rtnl1::YFP insertion (CPTI00291). (**C**–**E**) Confocal sections showing localization of Rtnl1::YFP in epidermal cells overlapping with KDEL (arrowheads in inset; C), in the larval ventral nerve cord (D) where it localizes preferentially in neuropil (arrow) and nerve bundles (arrowheads) in contrast to KDEL, which is concentrated within cell bodies (boxes), and in NMJ presynaptic boutons (E), where it follows the path of the axonal MT marker Futsch (upper panel). (**F**) VDRC RNAi line (construct GD900) successfully knocks down *Rtnl1* expression as observed by PCR amplification of *Rp49* and *Rtnl1* cDNA from progeny of *da-GAL4* crossed to either w^{1118} (control) or *Rtnl1* RNAi flies. (**G** and **H**) Loss of Rtnl1 causes an age-dependent climbing deficit. Graphs represent end-to-end distance travelled in 15 s (G) and climbing velocity (H) of *Rtnl1* RNAi and control flies (mean ± SEM here and in all subsequent graphs; $^{*}P < 0.05$, $^{**}P < 0.01$, $^{***}P < 0.005$, otherwise $P > 0.05$; two-way ANOVA and Bonferroni post-tests; $n = 3$ independent experiments).

which our earlier findings suggested localized to tubular ER compartments in axons. The highest probability Rtnl1::YFP interactor with predicted ER localization for which an antibody exists was Acyl-CoA synthestase (Acsl), the orthologue of human acyl-CoA synthetases 3 and 4 (34). In primary cultured mammalian neurons, Acsl4 localizes preferentially to tubular ER and is present in axons and dendrites (35,36). *Drosophila* Acsl staining, which follows long linear profiles within motor axon bundles, shows similar and overlapping localization to Rtnl1 in axons and epidermal cells (Fig. 3A and B). We confirmed by co-immunoprecipitation that Rtnl1 interacts with Acsl (Fig. 3C) and found that *Rtnl1* knockdown reduced Acsl protein levels compared with control larvae (Fig. 3D and E). Moreover, Acsl staining is selectively reduced in distal portions of the longer posterior abdominal motor axons, but not in the proximal portions of these axons (Fig. 3F).

Since Rtnl1::YFP also overlapped strongly with the MT marker Futsch in motor neuron terminals (Fig. 1F), we tested

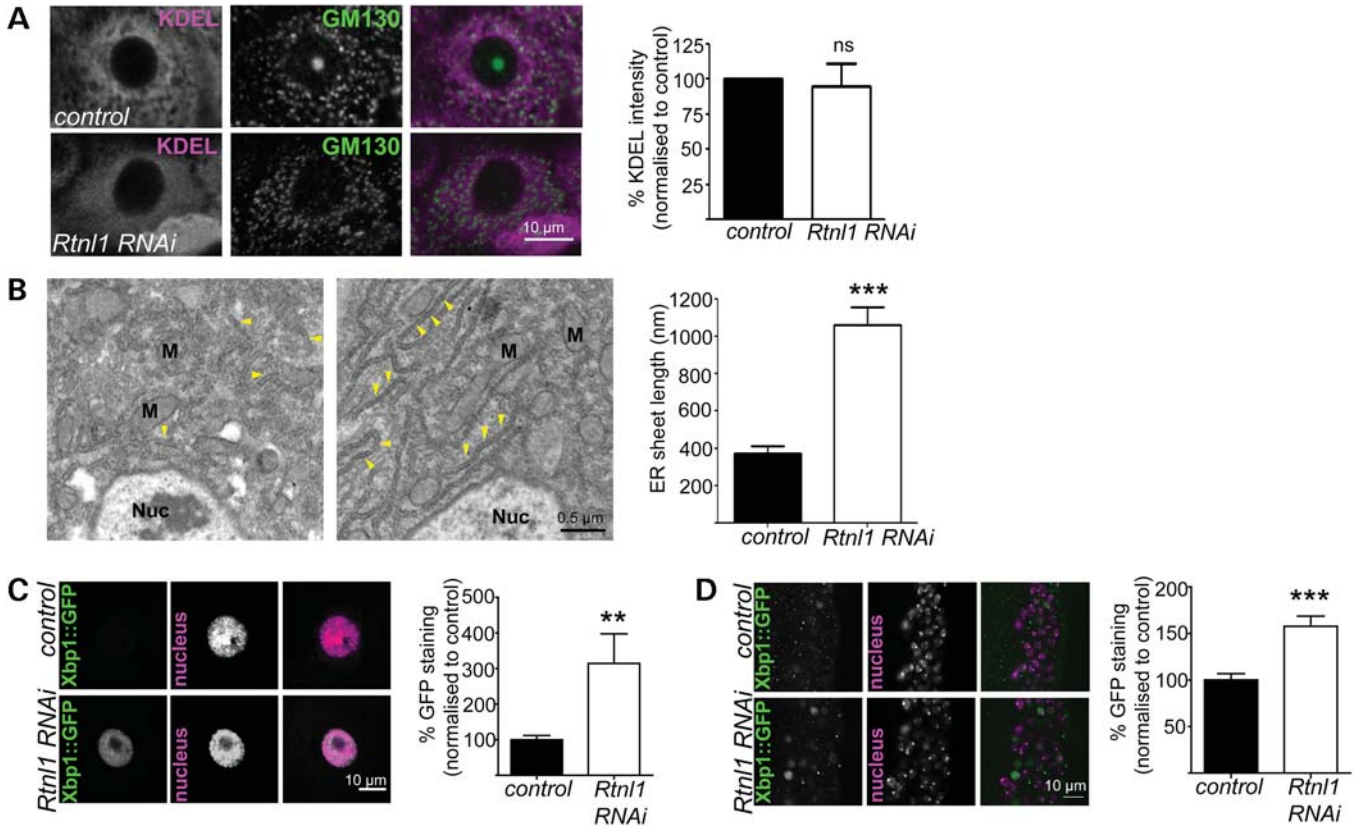

Figure 2. Loss of Rtnl1 causes expansion of ER sheets and increases the ER stress response. (**A**) KDEL distribution in third-instar larval epidermal cells is reticular in control larvae but more diffuse in *Rtnl1* RNAi larvae; distribution of the Golgi marker GM130 is broadly unaffected. Graph shows KDEL staining intensity per cell as a percentage of control levels ($n = 4$ independent experiments; ns, not significant, $P > 0.7$). (**B**) Electron micrographs show increased length of ER sheets in *Rtnl1* RNAi epidermal cells compared with controls. Arrowheads, ER sheets; Nuc, nucleus; M, mitochondrion. The graph shows the quantification of ER sheet cross-sectional length ($^{***}P < 0.005$; $n = 3$ independent larvae). (**C** and **D**) Single-confocal sections of larval epidermal cells (C) and ventral nerve cord (D) show increased ER stress, measured by increased Xbp1::GFP expression in *Rtnl1* RNAi larvae compared with controls and quantified in graphs ($^{**}P < 0.01$, $^{***}P < 0.005$; $n = 12–16$).

for effects of *Rtnl1* knockdown on the axonal cytoskeleton. Rtnl1::YFP could be co-immunoprecipitated with Futsch, suggesting that these proteins might interact directly or in a multiprotein complex (Fig. 4A). In *Rtnl1* knockdown larvae, overall levels of Futsch were approximately a third lower than in controls (Fig. 4B), and Futsch was preferentially lost from the distal portions of long motor axons in the posterior abdomen (Fig. 4C). Interestingly, *Acsl* mutants also lose Futsch staining from posterior NMJs and display a distal bias in axonal transport defects (37). Taken together, this could reflect an increased sensitivity of distal axons for tubular ER defects.

Loss of Rtnl1 causes disrupted mitochondrial organization in posterior NMJs

Since ER forms close contacts with mitochondria (38) and mutations in mitochondrial proteins may also cause HSP (39–41) as do RTN2 mutations (15), we also examined whether *Rtnl1* knockdown affected axonal or presynaptic mitochondria. *Rtnl1* knockdown did not cause a gross axon transport defect, as judged by axonal levels of the synaptic vesicle marker Csp and by numbers of mitochondria in axons (Fig. 5A). *Rtnl1* knockdown also had no effect on mitochondrial number or size in anterior abdominal NMJ boutons at muscles 6/7 (Fig. 5B). However, NMJ boutons at muscles 6/7 in the posterior abdomen contained fewer mitochondria, of greater size, in *Rtnl1* knockdown larvae than in controls (Fig. 5C). This suggests that the loss of Rtnl1 disrupts the localization or the fission/fusion balance of mitochondria in boutons of longer motor neurons.

DISCUSSION

The hairpin loop protein reticulon, along with REEP, atlastin and spastin family members, is required for ER network organization. The disruption of the ER network, brought about by mutations affecting any one of these families, results in the degeneration of long axons as observed in HSP. However, how mutations in these proteins can specifically target axonal degeneration is not understood. We describe a novel *Drosophila* model of HSP caused by loss of the orthologue of SPG12, *Rtnl1*. This is the first animal model providing evidence of an ER phenotype due to the loss of reticulon and shows that major rearrangements of ER morphology do not noticeably affect organismal survival. These findings are consistent with previous studies investigating reticulon function both in the yeast *Saccharomyces cervecisiae* and in the plant *Arabidopsis thaliana* (10,16,42,43). Importantly, our model also allows

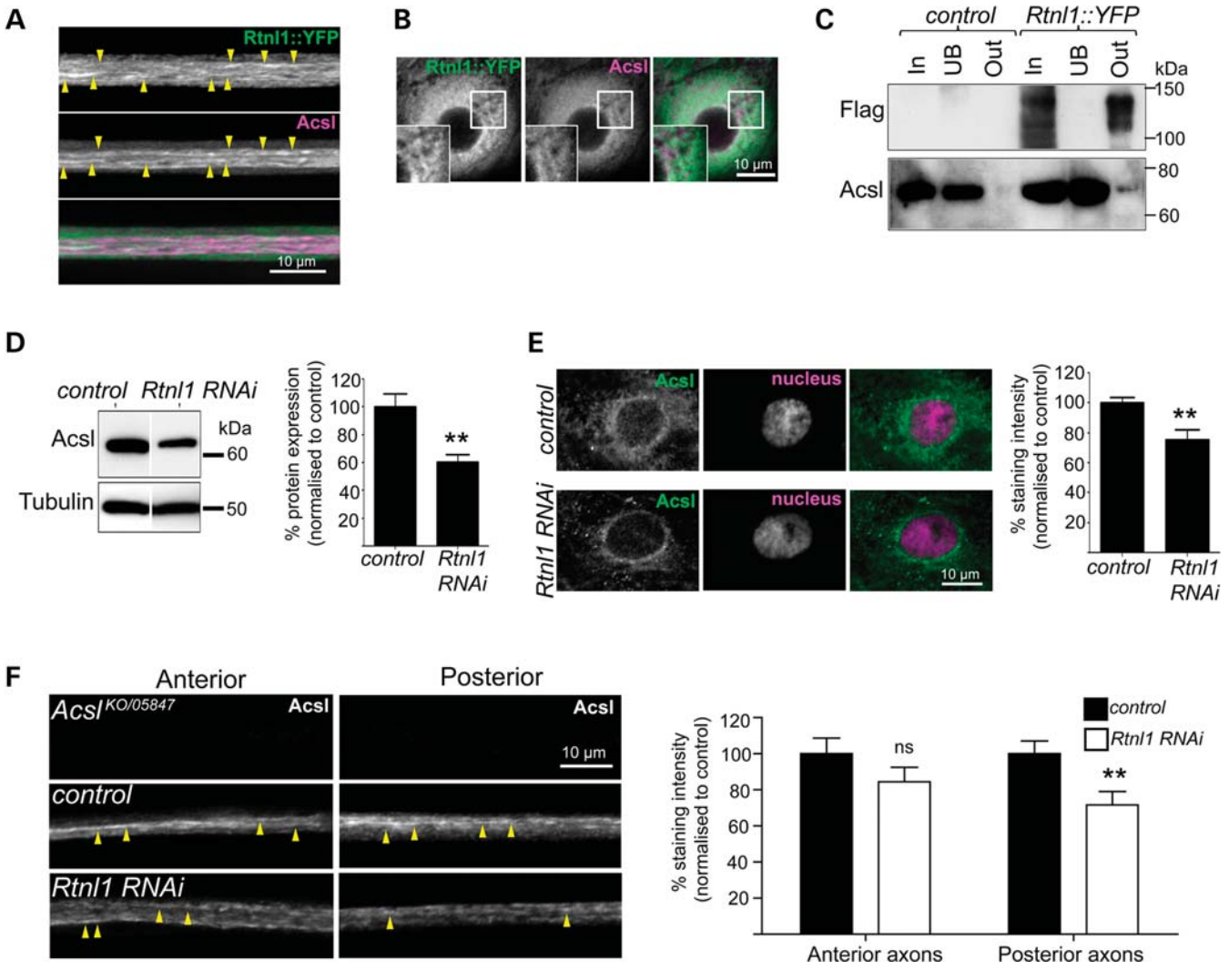

Figure 3. Rtnl1 interacts with the Acyl-CoA synthetase Acsl. Confocal sections showing overlapping localization of Rtnl1::YFP and Acsl in axons (linear staining indicated with arrowheads; **A**) and epidermal cells (**B**). (**C**) Protein lysates from *OregonR* (control) and *Rtnl1::YFP* flies were immunoprecipitated with Strep-Tactin Sepharose. Whole lysate (In), unbound (UB) and bound (Out) fractions were analysed by western blot. Loss of Rtnl1 reduces endogenous Acsl protein levels relative to controls in immunoblots of adult lysates (**D**) and single-confocal sections of larval epidermal cells (**E**). (**F**) Anti-Acsl staining of *OK6GAL4;UAS-Acsl::myc* motor neurons labels structures running along axons (arrowheads). Acsl staining is significantly lowered in posterior but not anterior segments of long motor axons upon knockdown of *Rtnl1* (F). Graphs represent Acsl expression levels (ns, not significant, $P > 0.2$; $^{**}P < 0.01$; $n = 6–8$ lysates in D, $n = 14–16$ larvae in E and F).

the investigation of the role of tubular ER in axons; the loss of Rtnl1 selectively effects longer axons, suggesting a mechanistic similarity between the cellular phenotypes of *Drosophila Rtnl1* knockdown and of spastic paraplegias that are caused by haplo-insufficient loss-of-function or dominant negative alleles of hairpin-loop proteins (15).

Although the disruption of SER functions, particularly in axons, is a prime candidate step to link the dysfunction of hairpin-loop HSP gene products to axon degeneration, studying the SER within axons has been challenging. In mature neurons, commonly used ER markers, including antibodies against KDEL (Fig. 1D) and PDI (21), localize preferentially to cell bodies rather than axons, likely reflecting the roles of these proteins in the protein biosynthetic region of the RER. However, Rtnl1::YFP and the tubular ER protein Acsl were highly expressed in mature motor axons. Here, they follow the distribution of axonal MT markers, reflecting the association of the ER with MTs (13,29). This association is required for the regulation of ER tubule dynamics via several mechanisms, the most common of which is ER sliding, whereby ER tubules bind to the shaft of an existing MT and slide along it as they grow (Fig. 6A) (38). Since the loss of *Rtnl1* leads to partial loss of the tubular ER marker Acsl specifically from the distal portions of longer motor axons, the loss or impairment of SER function in longer axons could underlie the axonal pathology of spastic paraplegia (Fig. 6B). We suggest that there may be only incomplete loss of tubular ER in *Rtnl1* knockdown axons due to partial functional redundancy between reticulon and other hairpin-loop family members, as occur in yeast (10).

Mitochondria and the ER have extensive contact points that are crucial for calcium homoeostasis and lipid biosynthesis (38). These contact points are mediated in part by the

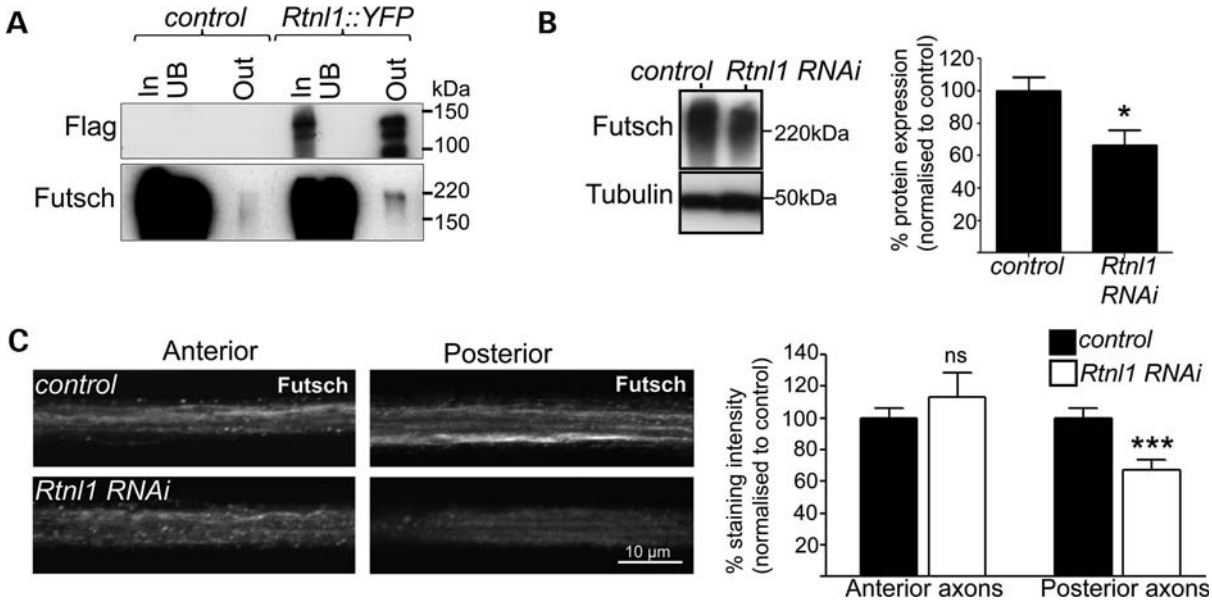

Figure 4. Rtnl1 interacts with the MT-associated protein Futsch. (**A**) Protein lysates from *OregonR* (control) and *Rtnl1::YFP* flies were immunoprecipitated and blotted as in Figure 3A. Loss of Rtnl1 reduces Futsch protein levels relative to controls in immunoblots of adult lysates (**B**) and in posterior but not anterior segments of long motor axons (**C**). Graphs represent Futsch expression levels (ns, not significant, $P > 0.44$; $^{*}P < 0.05$, $^{***}P < 0.001$; $n = 6–8$ lysates in B, $n = 16–19$ larvae in C).

mitochondrial fusion protein Mfn2 and are stably maintained during ER sliding along MTs (44,45). The loss of *Rtnl1* from motor neurons resulted in fewer, larger mitochondria within boutons of posterior, but not anterior, NMJs (Fig. 5). ER tubules appear to play a role in defining the position of mitochondrial division sites (46); therefore, mitochondrial fission at terminals of the longer motor axons could be more sensitive to ER tubule disruption, and the reduction in mitochondria in posterior axons could thus be a consequence of ER defects caused by loss of Rtnl1 (Fig. 6B). Furthermore, mitochondrial dysfunction is also implicated in some forms of HSP: mutations in a number of mitochondrial proteins can cause HSP (39–41); a number of other HSP proteins, spatacsin, spastizin and spartin (SPG11, SPG15 and SPG20, respectively) are reported to localize at least in part to mitochondria (47–49); and a possible mitochondrial fission defect has been reported in at least one SPG31 patient (50). Our observations indicate the possibility of mechanisms that may link the pathogenesis of HSP proteins involved in ER morphogenesis and mitochondrial dysfunction. It is worth noting however that in addition to mitochondria, the ER contacts other membranous organelles such as endosomes and mutlivesicular bodies as well as the plasma membrane (44,51,52). These interactions may also be affected by disruption of tubular ER.

Our results provide the first direct evidence of SER defects in mature axons in a loss-of-function SPG genotype. They also provide a route to further study the roles of the SER in normal neurons, impairment of which may lead to degeneration. These roles potentially include local effects on processes such as mitochondrial function and calcium homeostasis, but also long-distance communication along SER tubules, which extend throughout neurons, as in the 'neuron within a neuron' model (53). The study of HSP model flies in which SER organization is impaired promises to illuminate both the function of this fascinating compartment and the cell physiological processes that may be impaired by its disruption, and that may contribute to progressive axonal degeneration that spreads proximally from distal axonal ends.

MATERIALS AND METHODS

Fly stocks

The *Rtnl1* exon trap line *CPTI-001291* contains FLAG and StrepII tags in addition to Venus YFP (http://flybase.org/reports/FBal0262134.html). For knockdown experiments, either the *UAS-Rtnl1-RNAi* line 7866 (construct GD900, which has no predicted off-targets) or the w^{1118} control stock, 60000 (obtained from the Vienna *Drosophila* RNAi Center, www.vdrc.at) (54), was crossed with either *da-GAL4* (55) or *OK6-GAL4* (56); *da-GAL4* was used except where indicated otherwise. Other fly stocks used were *xbp1::EGFP* (33), *PBac{RB3.WH3}Acsl*^{KO} (37), *P{PZ}Acsl*^{05847} (34), *P{UAS-Acsl.715.MycC}3* (34) and mito::GFP (*P{UAS-mito-HA-GFP.AP}3*) (57).

Semi-quantitative PCR

Total RNA was purified from five male flies (<3 days post-eclosion) collected in TRIzol reagent (Invitrogen, Paisley, UK). cDNA was produced using the SuperScript III First Strand kit (Invitrogen, UK), 50 µM oligo-dT primer and 2 µg of DNase-treated RNA. Amplification of *Rp49* mRNA was used to control for cDNA concentration in the PCR reaction. Primers used were: Rp49-L: CCGACCACGTTACAAGAACTCTC; Rp49-R: CGCTTCAAGGGACAGTATCTGA; Rtnl1-L: ACGTAGGAGCACCGCGAACG; and Rtnl1-R: CTGAAGGCGACGGTGCCGAA. PCR conditions were

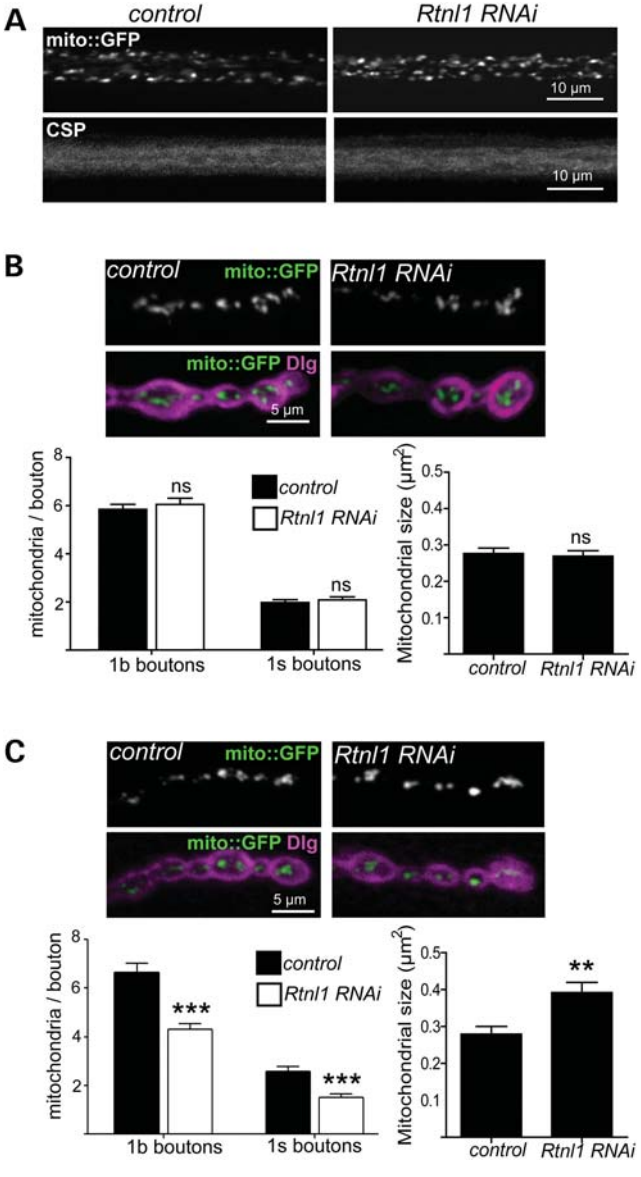

Figure 5. Effects of Rtnl1 loss on motor neuron mitochondria. (**A**) Single-confocal sections showing no effect of *Rtnl1* RNAi (generated using *OK6-GAL4* in this figure) on mito::GFP and CSP in posterior larval motor axons. (**B** and **C**) Single-confocal sections showing mito::GFP (green) and Dlg (magenta) at 1b boutons of anterior (B) and posterior (C) abdominal NMJs from control and *Rtnl1* RNAi larvae. Graphs show the number (in 1b and 1s boutons) and the size (in 1b boutons) of mitochondria in posterior NMJs (ns, not significant; $P > 0.5$, $^{**}P < 0.01$, $^{***}P < 0.0005$; $n = 18–22$ NMJs for 1b boutons, $n = 12$ NMJs for 1s boutons).

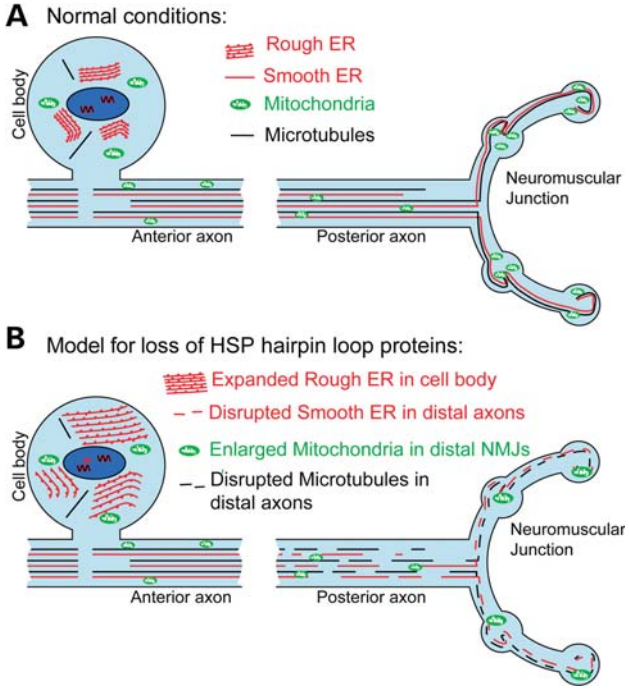

Figure 6. Model of hairpin loop protein dysfunction in motor neuron axonopathy. (**A**) The schematic diagram represents motor neurons under 'normal' or non-diseased conditions. Ribosomal studded RER sheets predominate within the neuronal cell body, whereas tubular SER runs the length of the axon closely associated with the MT cytoskeleton (13,21,29). In addition, the ER has extensive contact points with mitochondria which are required for lipid biosynthesis, calcium homeostasis and mitochondrial division (38,46). (**B**) Mutation or depletion of any one of the hairpin loop proteins causes disruption of the ER network (either less extensive and/or discontinuous) and degeneration of long motor axons as observed in HSP. Our findings have revealed an increased susceptibility of posterior axons to the disruption of ER organization, resulting in the disruption of tubular SER, MT cytoskeleton and mitochondria. This suggests that the loss of tubular ER from long motor axons may be the mechanism by which the loss of hairpin loop protein function gives rise to motor neuron axonopathy.

95°C for 30 s, 60°C for 30 s and 72°C for 1 min, repeated for 20 cycles for Rp49 and 25 cycles for Rtnl1. At least six different samples for each genotype were analysed. PCR products were visualized with ethidium bromide on a gel, and band intensities quantified using ImageJ.

Immunoprecipitation and immunoblot

Soluble protein lysates were purified from male flies (<3 days post-eclosion) by homogenization in 1% Triton X-100, 25 mM HEPES (pH 7.4), 150 mM NaCl, 2 mM EDTA and Protease Inhibitor Cocktail (Sigma, Poole, UK), followed by centrifugation at 15 000*g* for 30 min at 4°C. Immunoprecipitation was carried out with Strep-Tactin Sepharose (IBA, Göttingen, Germany). Briefly, protein samples (Input) were incubated overnight at 4°C with Strep-Tactin Sepharose, and unbound and bound proteins were collected by centrifugation. For immunoblot, protein samples were separated on polyacrylamide minigels and electrophoretically transferred to nitrocellulose membranes (Bio-Rad, Hercules, CA, USA). The nitrocellulose was blocked in 5% non-fat milk in 10 mM Tris–HCl, 100 mM NaCl and 0.05% Tween-20 and incubated with primary antibodies overnight at 4°C. Primary antibodies used were against: FLAG (F1804; Sigma), Acsl (34), α-tubulin (T9026; Sigma) and Futsch (22C10; Hybridoma) (58). After incubation with HRP (horseradish peroxidase)-coupled secondary antibodies and SuperSignal Chemiluminescent Substrate (Pierce), bands were visualized by autoradiography. Band intensities were determined using ImageJ, and levels from knockdown samples normalized to control samples on the same film.

Histology and immunomicroscopy

Third-instar larvae were dissected in chilled Ca^{2+}-free HL3 solution (59), fixed in 4% formaldehyde in PBS for 30 min and permeabilized in 0.1% Triton X-100 in PBS. Primary antibodies used were as for immunoblotting and against: GFP (ab6556; Abcam, Cambridge, UK), KDEL (MAC256; Abcam), GM130 (Ab32337; Abcam), HRP (P7899; Sigma), Discs-large (4F3) (60) and cysteine string protein (DCSP-2 (6D6) (61). The nuclear stain used was TO-PRO-3 iodide (T3605; Invitrogen). Fixed preparations were mounted in Vectashield (Vector Laboratories) and viewed using a Nikon CSi confocal head mounted on an Eclipse 90i microscope. Motor axons were imaged passing through segment A2 ('anterior') and segment A6 ('posterior'). NMJs were imaged at muscle 6/7 of segment A3 ('anterior') and segment A6 ('posterior'). Images were acquired using a 60×/1.4NA objective and the Nikon EZC1 3.90 software, and imported to ImageJ. Brightness, contrast and colour channels were adjusted using Photoshop (Adobe).

Image analysis

For fluorescence intensity analysis, control and mutant larvae were stained and washed in the same tube, with one genotype tail-clipped for identification. Mean grey intensity for regions of interest was quantified in ImageJ, using at least three independent experiments, each with at least four larvae. Mitochondria were counted manually, blind to genotype. Type 1b and 1s boutons were differentiated by intensity of Dlg staining.

Electron microscopy

Third-instar larvae were dissected in chilled Ca^{2+}-free HL3 solution and fixed in 3% glutaraldehyde, 0.3% hydrogen peroxide and 2 mM sodium EDTA for 4 h at 4°C. After four washes in 0.1 M HEPES buffer, larva were post-fixed in 1% osmium ferricyanide (Oxchem, Edinburgh, UK) in buffer at room temperature for 1 h. After rinsing in de-ionized water, samples were stained in 2% uranyl acetate in maleate buffer, dehydrated in an ethanol series, followed by acetonitrile and then infiltrated with Quetol epoxy resin (Agar Scientific, Stansted, UK) and cured at 60°C for 48 h. Sections were cut on a Leica Ultracut UCT ultra-microtome at 70 nm, using a diamond knife, and contrasted with uranyl acetate and lead citrate. They were viewed using a Tecnai G2 electron microscope operated at 120 kV, and an AMT XR60B camera running the Deben software. EM images were collected from three larvae per genotype, with at least five epidermal cells imaged per larva. Images were blinded for genotype before ER branch length was determined in ImageJ.

Locomotor assay

Locomotor assays were carried out as described (30), using 10 flies per vial, 3 vials per experiment and 3 independent experiments. Flies were kept at 25°C and assayed every 3 days. Climbing ability was determined over 15 s in a vertical glass vial (10 cm length, 2.5 cm diameter). All trajectories were quantified for their end-to-end distance and their velocity.

Statistical analysis

Data were exported to GraphPad Prism 5 (GraphPad Software, Inc.) for statistical analysis. Statistical significance was determined using Student's *t*-test, except for analysis of climbing, where two-way ANOVA and Bonferroni *post hoc* analyses were used.

ACKNOWLEDGEMENTS

We thank Z. Wang, H.D. Ryoo, T.E. Rusten, J. Roote, the Developmental Studies Hybridoma Bank and the Bloomington and Vienna *Drosophila* Stock Centres for antibodies and stocks. We thank J. Skepper and J. Powell for help with EM, K. Lilley for support with mass spectrometry analysis, and D. Crowther and A. Mok for assistance with the fly climbing assay.

Conflict of Interest statement. None declared.

FUNDING

N.C.O'S. was supported by Marie Curie Individual Fellowship 236777. E.R. is a Wellcome Trust Senior Research Fellow in Clinical Science (grant 082381) and is supported by a strategic award from the Wellcome Trust to CIMR (grant 079895). Funding to pay the Open Access publication charges for this article was provided by the Wellcome Trust.

REFERENCES

1. Reid, E. (2003) Science in motion: common molecular pathological themes emerge in the hereditary spastic paraplegias. *J. Med. Genet.*, **40**, 81–86.
2. Fink, J.K. (2006) Hereditary spastic paraplegia. *Curr. Neurol. Neurosci. Rep.*, **6**, 65–76.
3. Blackstone, C., O'Kane, C.J. and Reid, E. (2011) Hereditary spastic paraplegias: membrane traffic and the motor pathway. *Nat. Rev. Neurosci.*, **12**, 31–42.
4. Wang, X., Shaw, W.R., Tsang, H.T., Reid, E. and O'Kane, C.J. (2007) *Drosophila* spichthyin inhibits BMP signaling and regulates synaptic growth and axonal microtubules. *Nat. Neurosci.*, **10**, 177–185.
5. Tsang, H.T., Edwards, T.L., Wang, X., Connell, J.W., Davies, R.J., Durrington, H.J., O'Kane, C.J., Luzio, J.P. and Reid, E. (2009) The hereditary spastic paraplegia proteins NIPA1, spastin and spartin are inhibitors of mammalian BMP signalling. *Hum. Mol. Genet.*, **18**, 3805–3821.
6. Fassier, C., Hutt, J.A., Scholpp, S., Lumsden, A., Giros, B., Nothias, F., Schneider-Maunoury, S., Houart, C. and Hazan, J. (2010) Zebrafish atlastin controls motility and spinal motor axon architecture via inhibition of the BMP pathway. *Nat. Neurosci.*, **13**, 1380–1387.
7. Szymanski, K.M., Binns, D., Bartz, R., Grishin, N.V., Li, W.P., Agarwal, A.K., Garg, A., Anderson, R.G. and Goodman, J.M. (2007) The lipodystrophy protein seipin is found at endoplasmic reticulum lipid droplet junctions and is important for droplet morphology. *Proc. Natl Acad. Sci. USA*, **104**, 20890–20895.
8. Eastman, S.W., Yassaee, M. and Bieniasz, P.D. (2009) A role for ubiquitin ligases and Spartin/SPG20 in lipid droplet turnover. *J. Cell Biol.*, **184**, 881–894.
9. Edwards, T.L., Clowes, V.E., Tsang, H.T., Connell, J.W., Sanderson, C.M., Luzio, J.P. and Reid, E. (2009) Endogenous spartin (SPG20) is recruited to endosomes and lipid droplets and interacts with the ubiquitin E3 ligases AIP4 and AIP5. *Biochem. J.*, **423**, 31–39.
10. Voeltz, G.K., Prinz, W.A., Shibata, Y., Rist, J.M. and Rapoport, T.A. (2006) A class of membrane proteins shaping the tubular endoplasmic reticulum. *Cell*, **124**, 573–586.

11. Hu, J., Shibata, Y., Voss, C., Shemesh, T., Li, Z., Coughlin, M., Kozlov, M.M., Rapoport, T.A. and Prinz, W.A. (2008) Membrane proteins of the endoplasmic reticulum induce high-curvature tubules. *Science*, **319**, 1247–1250.
12. Orso, G., Pendin, D., Liu, S., Tosetto, J., Moss, T.J., Faust, J.E., Micaroni, M., Egorova, A., Martinuzzi, A., McNew, J.A. and Daga, A. (2009) Homotypic fusion of ER membranes requires the dynamin-like GTPase atlastin. *Nature*, **460**, 978–983.
13. Park, S.H., Zhu, P.P., Parker, R.L. and Blackstone, C. (2010) Hereditary spastic paraplegia proteins REEP1, spastin, and atlastin-1 coordinate microtubule interactions with the tubular ER network. *J. Clin. Invest.*, **120**, 1097–1110.
14. Hu, J., Shibata, Y., Zhu, P.P., Voss, C., Rismanchi, N., Prinz, W.A., Rapoport, T.A. and Blackstone, C. (2009) A class of dynamin-like GTPases involved in the generation of the tubular ER network. *Cell*, **138**, 549–561.
15. Montenegro, G., Rebelo, A.P., Connell, J., Allison, R., Babalini, C., D'Aloia, M., Montieri, P., Schüle, R., Ishiura, H., Price, J. *et al.* (2012) Mutations in the ER-shaping protein human Reticulon2 cause axonal degeneration in hereditary spastic paraplegia type 12. *J. Clin. Invest.*, **122**, 538–544.
16. Shibata, Y., Shemesh, T., Prinz, W.A., Palazzo, A.F., Kozlov, M.M. and Rapoport, T.A. (2010) Mechanisms determining the morphology of the peripheral ER. *Cell*, **143**, 774–788.
17. Evans, K.J., Gomes, E.R., Reisenweber, S.M., Gundersen, G.G. and Lauring, B.P. (2005) Linking axonal degeneration to microtubule remodeling by Spastin-mediated microtubule severing. *J. Cell Biol.*, **168**, 599–606.
18. Roll-Mecak, A. and Vale, R.D. (2005) The *Drosophila* homologue of the hereditary spastic paraplegia protein, spastin, severs and disassembles microtubules. *Curr. Biol.*, **15**, 650–655.
19. Sanderson, C.M., Connell, J.W., Edwards, T.L., Bright, N.A., Duley, S., Thompson, A., Luzio, J.P. and Reid, E. (2006) Spastin and atlastin, two proteins mutated in autosomal-dominant hereditary spastic paraplegia, are binding partners. *Hum. Mol. Genet.*, **15**, 307–318.
20. Bian, X., Klemm, R.W., Liu, T.Y., Zhang, M., Sun, S., Sui, X., Liu, X., Rapoport, T.A. and Hu, J. (2011) Structures of the atlastin GTPase provide insight into homotypic fusion of endoplasmic reticulum membranes. *Proc. Natl Acad. Sci. USA*, **108**, 3976–3981.
21. Rolls, M.M., Hall, D.H., Victor, M., Stelzer, E.H. and Rapoport, T.A. (2002) Targeting of rough endoplasmic reticulum membrane proteins and ribosomes in invertebrate neurons. *Mol. Cell. Biol.*, **13**, 1787–1791.
22. Rolls, M.M., Satoh, D., Clyne, P.J., Henner, A.L., Uemura, T. and Doe, C.Q. (2007) Polarity and intracellular compartmentalization of *Drosophila* neurons. *Neural Dev.*, **2**, 7.
23. Broadwell, R.D. and Cataldo, A.M. (1984) The neuronal endoplasmic reticulum: its cytochemistry and contribution to the endomembrane system. *J. Comp. Neurol.*, **230**, 231–248.
24. Burton, P.R. and Laveri, L.A. (1985) The distribution, relationships to other organelles, and calcium-sequestering ability of smooth endoplasmic reticulum in frog olfactory axons. *J. Neurosci.*, **5**, 3047–3060.
25. Hartter, D.E., Burton, P.R. and Laver, L.A. (1987) Distribution and calcium-sequestering ability of smooth endoplasmic reticulum in olfactory axon terminals of frog brain. *Neurosci.*, **23**, 371–386.
26. Shimizu, H., Fukaya, M., Yamasaki, M., Watanabe, M., Manabe, T. and Kamiya, H. (2008) Use-dependent amplification of presynaptic Ca2+ signaling by axonal ryanodine receptors at the hippocampal mossy fiber synapse. *Proc. Natl Acad. Sci. USA*, **105**, 11998–12003.
27. Wakefield, S. and Tear, G. (2006) The *Drosophila* reticulon, Rtnl-1, has multiple differentially expressed isoforms that are associated with a sub-compartment of the endoplasmic reticulum. *Cell. Mol. Life Sci.*, **63**, 2027–2038.
28. Röper, K. (2007) Rtnl1 is enriched in a specialized germline ER that associates with ribonucleoprotein granule components. *J. Cell Sci.*, **120**, 1081–1092.
29. Waterman-Storer, C.M. and Salmon, E.D. (1998) Endoplasmic reticulum membrane tubules are distributed by microtubules in living cells using three distinct mechanisms. *Curr. Biol.*, **8**, 798–806.
30. Jahn, T.R., Kohlhoff, K.J., Scott, M., Tartaglia, G.G., Lomas, D.A., Dobson, C.M., Vendruscolo, M. and Crowther, D.C. (2011) Detection of early locomotor abnormalities in a *Drosophila* model of Alzheimer's disease. *J. Neurosci. Methods*, **197**, 186–189.
31. Ron, D. and Walter, P. (2007) Signal integration in the endoplasmic reticulum unfolded protein response. *Nat. Rev. Mol. Cell Biol.*, **8**, 519–529.
32. Sriburi, R., Jackowski, S., Mori, K. and Brewer, J.W. (2004) XBP1: a link between the unfolded protein response, lipid biosynthesis, and biogenesis of the endoplasmic reticulum. *J. Cell Biol.*, **167**, 35–41.
33. Ryoo, H.D., Domingos, P.M., Kang, M.J. and Steller, H. (2007) Unfolded protein response in a *Drosophila* model for retinal degeneration. *EMBO J.*, **26**, 242–252.
34. Zhang, Y., Chen, D. and Wang, Z. (2009) Analyses of mental dysfunction-related ACSl4 in *Drosophila* reveal its requirement for Dpp/BMP production and visual wiring in the brain. *Hum. Mol. Genet.*, **18**, 3894–3905.
35. Piccini, M., Vitelli, F., Bruttini, M., Pober, B.R., Jonsson, J.J., Villanova, M., Zollo, M., Borsani, G., Ballabio, A. and Renieri, A. (1998) FACL4, a new gene encoding long-chain acyl-CoA synthetase 4, is deleted in a family with Alport syndrome, elliptocytosis, and mental retardation. *Genomics*, **47**, 350–358.
36. Meloni, I., Parri, V., De Filippis, R., Ariani, F., Artuso, R., Bruttini, M., Katzaki, E., Longo, I., Mari, R., Bellan, C. *et al.* (2009) The XLMR gene *ACSL4* plays a role in dendritic spine architecture. *Neuroscience*, **159**, 657–669.
37. Liu, Z., Huang, Y., Zhang, Y., Chen, D. and Zhang, Y.Q. (2011) *Drosophila* Acyl-CoA synthetase long-chain family member 4 regulates axonal transport of synaptic vesicles and is required for synaptic development and transmission. *J. Neurosci.*, **31**, 2052–2063.
38. de Brito, O.M. and Scorrano, L. (2010) An intimate liaison: spatial organization of the endoplasmic reticulum–mitochondria relationship. *EMBO J.*, **29**, 2715–2723.
39. Casari, G., De Fusco, M., Ciarmatori, S., Zeviani, M., Mora, M., Fernandez, P., De Michele, G., Filla, A., Cocozza, S., Marconi, R., Dürr, A. *et al.* (1998) Spastic paraplegia and OXPHOS impairment caused by mutations in paraplegin, a nuclear-encoded mitochondrial metalloprotease. *Cell*, **93**, 973–983.
40. Hansen, J.J., Dürr, A., Cournu-Rebeix, I., Georgopoulos, C., Ang, D., Nielsen, M.N., Davoine, C.S., Brice, A., Fontaine, B., Gregersen, N. and Bross, P. (2002) Hereditary spastic paraplegia SPG13 is associated with a mutation in the gene encoding the mitochondrial chaperonin Hsp60. *Am. J. Hum. Genet.*, **70**, 1328–1332.
41. Verny, C., Guegen, N., Desquiret, V., Chevrollier, A., Prundean, A., Dubas, F., Cassereau, J., Ferre, M., Amati-Bonneau, P., Bonneau, D. *et al.* (2011) Hereditary spastic paraplegia-like disorder due to a mitochondrial ATP6 gene point mutation. *Mitochondrion*, **11**, 70–75.
42. Tolley, N., Sparkes, I.A., Hunter, P.R., Craddock, C.P., Nuttall, J., Roberts, L.M., Hawes, C., Pedrazzini, E. and Frigerio, L. (2008) Overexpression of a plant reticulon remodels the lumen of the cortical endoplasmic reticulum but does not perturb protein transport. *Traffic*, **9**, 94–102.
43. Sparkes, I., Tolley, N., Aller, I., Svozil, J., Osterrieder, A., Botchway, S., Mueller, C., Frigerio, L. and Hawes, C. (2010) Five *Arabidopsis* reticulon isoforms share endoplasmic reticulum location, topology, and membrane-shaping properties. *Plant Cell*, **22**, 1333–1343.
44. Friedman, J.R., Webster, B.M., Mastronarde, D.N., Verhey, K.J. and Voeltz, G.K. (2010) ER sliding dynamics and ER-mitochondrial contacts occur on acetylated microtubules. *J. Cell Biol.*, **190**, 363–375.
45. de Brito, O.M. and Scorrano, L. (2008) Mitofusin 2 tethers endoplasmic reticulum to mitochondria. *Nature*, **456**, 605–610.
46. Friedman, J.R., Lackner, L.L., West, M., DiBenedetto, J.R., Nunnari, J. and Voeltz, G.K. (2011) ER tubules mark sites of mitochondrial division. *Science*, **334**, 358–362.
47. Lu, J., Rashid, F. and Byrne, P.C. (2006) The hereditary spastic paraplegia protein spartin localises to mitochondria. *J. Neurochem.*, **98**, 1908–1919.
48. Murmu, R.P., Martin, E., Rastetter, A., Esteves, T., Muriel, M.P., El Hachimi, K.H., Denora, P.S., Dauphin, A., Fernandez, J.C., Duyckaerts, C. *et al.* (2011) Cellular distribution and subcellular localization of spatacsin and spastizin, two proteins involved in hereditary spastic paraplegia. *Mol. Cell. Neurosci.*, **47**, 191–202.
49. Yao, A., Jin, S., Li, X., Liu, Z., Ma, X., Tang, J. and Zhang, Y.Q. (2011) *Drosophila* FMRP regulates microtubule network formation and axonal transport of mitochondria. *Hum. Mol. Genet.*, **20**, 51–63.
50. Goizet, C., Depienne, C., Benard, G., Boukhris, A., Mundwiller, E., Sole, G., Coupry, I., Pilliod, J., Martin-Negrier, M., Fedirko, E. *et al.* (2011) REEP1 mutations in SPG31: frequency, mutational spectrum, and

potential association with mitochondrial morpho-functional dysfunction. *Hum. Mutat.*, **32**, 1118–1127.
51. Wu, M.M., Buchanan, J., Luik, R.M. and Lewis, R.S. (2006) Ca2+ store depletion causes STIM1 to accumulate in ER regions closely associated with the plasma membrane. *J. Cell Biol.*, **174**, 803–813.
52. Eden, E.R., White, I.J., Tsapara, A. and Futter, C.E. (2010) Membrane contacts between endosomes and ER provide sites for PTP1B-epidermal growth factor receptor interaction. *Nat. Cell Biol.*, **12**, 267–272.
53. Berridge, M.J. (1998) Neuronal calcium signalling. *Neuron*, **21**, 13–26.
54. Dietzl, G., Chen, D., Schnorrer, F., Su, K.C., Barinova, Y., Fellner, M., Gasser, B., Kinsey, K., Oppel, S., Scheiblauer, S. *et al.* (2007) A genome-wide transgenic RNAi library for conditional gene inactivation in *Drosophila*. *Nature*, **448**, 151–156.
55. Perrin, L., Bloyer, S., Ferraz, C., Agrawal, N., Sinha, P. and Dura, J.M. (2003) The leucine zipper motif of the *Drosophila* AF10 homologue can inhibit PRE-mediated repression: implications for leukemogenic activity of human MLL-AF10 fusions. *Mol. Cell. Biol.*, **23**, 119–130.
56. Aberle, H., Haghighi, A.P., Fetter, R.D., McCabe, B.D., Magalhaes, T.R. and Goodman, C.S. (2002) wishful thinking encodes a BMP type II receptor that regulates synaptic growth in *Drosophila*. *Neuron*, **33**, 545–558.
57. Pilling, A.D., Horiuchi, D., Lively, C.M. and Saxton, W.M. (2006) Kinesin-1 and Dynein are the primary motors for fast transport of mitochondria in *Drosophila* motor axons. *Mol. Biol. Cell*, **17**, 2057–2068.
58. Fujita, S.C., Zipursky, S.L., Benzer, S., Ferrus, A. and Shotwell, S.L. (1982) Monoclonal antibodies against the *Drosophila* nervous system. *Proc. Natl Acad. Sci. USA*, **79**, 7929–7933.
59. Stewart, B.A., Atwood, H.L., Renger, J.J., Wang, J. and Wu, C.F. (1994) Improved stability of *Drosophila* larval neuromuscular preparations in haemolymph-like physiological solutions. *J. Comp. Physiol. A.*, **175**, 179–191.
60. Parnas, D., Haghighi, A.P., Fetter, R.D., Kim, S.W. and Goodman, C.S. (2001) Regulation of postsynaptic structure and protein localization by the Rho-type guanine nucleotide exchange factor dPix. *Neuron*, **32**, 415–424.
61. Zinsmaier, K.E., Eberle, K.K., Buchner, E., Walter, N. and Benzer, S. (1994) Paralysis and early death in cysteine string protein mutants of *Drosophila*. *Science*, **263**, 977–980.